Inferring the effects of sink strength on plant carbon balance processes from experimental measurements

Kashif Mahmud[1], Belinda E. Medlyn[1], Remko A. Duursma[1], Courtney Campany[1,2], Martin G. De Kauwe[3]

[1]Hawkesbury Institute for the Environment, Western Sydney University, Locked Bag 1797, Penrith NSW 2751, Australia

[2]Department of Biology, Colgate University, NY 13346, USA

[3]ARC Centre of Excellence for Climate Extremes, University of New South Wales, Sydney, NSW 2052, Australia

Correspondence to: Kashif Mahmud (k.mahmud@westernsydney.edu.au)

Abstract

The lack of correlation between photosynthesis and plant growth under sink-limited conditions is a long-standing puzzle in plant ecophysiology that currently severely compromises our models of vegetation responses to global change. To address this puzzle, we applied data assimilation to an experiment where sink strength of *Eucalyptus tereticornis* seedlings were manipulated by restricting root volume. Our goals were to infer which processes were affected by sink limitation, and to attribute the overall reduction in growth observed in the experiment, to the effects on various carbon (C) component processes. Our analysis was able to infer that, in addition to a reduction in photosynthetic rates, sink limitation reduced the rate of utilization of non-structural carbohydrate (NSC), enhanced respiratory losses, modified C allocation and increased foliage turnover. Each of these effects was found to have a significant impact on final plant biomass accumulation. We also found that inclusion of a NSC storage pool was necessary to capture seedling growth over time, particularly for sink limited seedlings. Our approach of applying data assimilation to infer C balance processes in a manipulative experiment enabled us to extract new information on the timing, magnitude, and direction of the internal C fluxes from an existing dataset. We suggest

this approach could, if used more widely, be an invaluable tool to develop appropriate representations of sink-limited growth in terrestrial biosphere models.

Keywords: Non-structural carbohydrate, carbon allocation, data assimilation, mass-balance, photosynthesis, plant growth, sink regulation

1 Introduction

Almost all mechanistic models of terrestrial vegetation function are based on the carbon (C) balance: plant growth is represented as the difference between C uptake (through photosynthesis) and C loss (through respiration and turnover of plant parts). This approach to modeling plant growth dates back to early crop and forest production models (McMurtrie and Wolf, 1983; de Wit and van Keulen, 1987; de Wit, 1978) and now provides the fundamental quantitative framework to integrate our scientific understanding of plant ecosystem function (Makela et al., 2000).

However, C balance models have been criticized for being "source-focused" (Fatichi et al., 2014). Most C balance models predict growth from the environmental responses of photosynthesis ("source limitation"). In contrast to this assumption, many experimental studies demonstrate that growth is directly limited by environmental conditions ("sink limitation") rather than the availability of photosynthate. For example, growth is more sensitive to water limitation than is photosynthesis (Bradford and Hsiao, 1982; Müller et al., 2011; Mitchell et al., 2014); low temperatures are considerably more limiting to cell division than to photosynthesis (Körner et al., 2014); nutrient limitation may slow growth without reducing photosynthesis (Reich, 2012; Crous and Ellsworth, 2004); and, physical sink-limitation may reduce growth with a decline in photosynthetic capacity and an accumulation of leaf starch (Arp, 1991; Campany et al., 2017; Poorter et al., 2012a; Paul and Foyer, 2001).

How can we move to models that include both source- and sink-limitation? There is ongoing discussion about realistic implementations of non-structural carbohydrates (NSC) in vegetation models because of their multiple roles in plant functioning, such an implementation provides a buffer against discrepancies in source and sink activity. Some C

balance models include a "storage" pool of NSC (Running and Gower, 1991; Bossel, 1996; Thornley and Cannell, 2000), but most of these models make the assumption that the NSC pool acts merely as a buffer between C sources and sinks, balancing out seasonally or at least over several seasons (Fatichi et al., 2014; Friend et al., 2014; De Kauwe et al., 2014; Schiestl-Aalto et al., 2015). There is mounting evidence that the NSC plays a more active role in tree physiology (Buckley, 2005; Sala et al., 2012; Wiley and Helliker, 2012; Hartmann et al., 2015). For example, NSC accumulation can lead to down-regulation of photosynthesis (Nikinmaa et al., 2014). Therefore, the need to quantify the NSC pool and to better understand the prioritisation of storage vs. growth is of great importance.

An understanding of the dynamics of storage is also essential to correctly represent the C balance in models (Hartmann and Trumbore, 2016). If, for example, a direct growth limitation is implemented into models, how should the surplus of accumulated photosynthates be treated? In their proof-of-concept sink-limited model, Fatichi et al. (2014) allowed reserves to accumulate indefinitely. Alternatively, some models (e.g. CABLE (Law et al., 2006), O-CN (Zaehle and Friend, 2010)) increase respiration rates when excess labile C accumulates. Both approaches can be seen as model-oriented solutions to maintain C balance that are unsatisfactory because they are not based on empirical data. Experiments where sink strength is manipulated may provide the key to improve our understanding of C balance processes under direct growth limitation.

Efforts have been made to understand the physiological and morphological changes in response to belowground C sink limitation by manipulating rooting volume in tree seedlings (Arp, 1991; Campany et al., 2017; Poorter et al., 2012a). These experiments often reveal photosynthetic down-regulation and accumulation of leaf starch, and reductions in growth (Arp, 1991; McConnaughay and Bazzaz, 1991; Gunderson and Wullschleger, 1994; Sage, 1994; Poorter et al., 2012a; Robbins and Pharr, 1988; Maina et al., 2002; Campany et al., 2017). In a recent study with Eucalyptus seedlings, Campany et al. (2017) showed that the reduction in seedling growth when rooting volume was restricted could not be completely explained by the negative effects of sink limitation on photosynthesis, suggesting that other components of the C balance were affected in the process. However, Campany et al. (2017) could not accurately quantify all components of tree C balance, i.e. photosynthesis, carbohydrate storage, biomass partitioning and respiration.

89 Quantifying all components of C balance is not an easy task, given that not all processes are
90 measured with equal fidelity, and data gaps will always occur. Klein and Hoch (2015) used a
91 C mass balance approach with a tabular process flowchart to decipher C components and
92 provide a full description of tree C allocation dynamics. Here, rather than using a manual
93 process, we used a data assimilation (DA)-modelling framework, which has been proven to
94 be a powerful tool in analyzing complex C balance problems (Williams et al., 2005;
95 Richardson et al., 2013). For example, Richardson et al. (2013) use DA to discriminate
96 among alternative models for the dynamics of non-structural carbon (NSC), finding that a
97 model with two NSC pools, fast and slow, performed best; Rowland et al. (2014) applied DA
98 to experimental observations of ecosystem C stocks and fluxes to infer seasonal shifts in C
99 allocation and plant respiration in an Amazon forest; and Bloom et al. (2016) used DA to
100 constrain a C balance model with satellite-derived measurements of leaf C, to simulate
101 continental-scale patterns in C cycle processes.

102 Our goal in this paper was to use DA to quantify the impact of sink limitation on C balance
103 processes. We utilized data from an experiment in which sink limitation was induced by
104 restricting the rooting volume of *Eucalyptus tereticornis* seedlings over the course of 4
105 months (Campany et al., 2017). We assimilated photosynthesis and growth measurements
106 from the experiment into a simple C balance model, to infer the effects of sink limitation on
107 the main C balance processes, namely: respiration, carbohydrate utilization, allocation, and
108 turnover.

109 Although in reality plants do have a storage component, it is not necessarily the case that
110 including such a storage component in the model leads to model improvement. Hence, it is
111 important to test whether or not adding the storage component improves the performance of
112 the model enough to justify the additional complexity. Therefore, we first tested two null
113 hypotheses:

114 H1: There is no need to consider storage in the model: growth can be adequately predicted
115 from current day photosynthate.

116 H2: There is no effect of sink limitation on C balance processes other than via a reduction of
117 photosynthesis.

118 We were then interested to test the following specific hypotheses about the impact of sink
119 limitation on C balance:

H3: We hypothesized that the rate of utilization of carbohydrate for plant growth would be lower under sink limitation, causing growth rates to slow and non-structural carbohydrate to accumulate.

H4: We hypothesized that under sink limitation a larger proportion of C would be lost to growth respiration and less used for production. We have dubbed this the "wasteful plant" hypothesis; this hypothesis corresponds to the assumption embedded in some models that respiration is up-regulated when labile C accumulates e.g. CABLE, O-CN (Law et al., 2006; Zaehle and Friend, 2010).

H5: We hypothesized that foliage and root C allocation fractions would be reduced, in favour of wood allocation. Sink limitation induced by nutrient and/or water stress often results in a shift in C allocation away from foliage and towards fine roots (Poorter et al., 2012b). However, for this experiment, the physical restriction of root growth limits the potential for root allocation. Hence, we predicted that both foliage and fine root allocation would decrease.

2 Materials and Methods

2.1 Experiment description

The site and experimental setup have been described in detail by Campany et al. (2017), so we only provide a brief description here. The experiment was carried out at the Hawkesbury Forest Experiment site (33°37'S 150°44'E) in Richmond, NSW, Australia. The site is located in the sub-humid temperate region and experiences warm summers and cool winters. The seedlings were planted on 21st January 2013 (mid-summer) and harvested on 21st May 2013 (late autumn). Mean daily temperatures ranged from 22.8 to 46.4 °C (monthly mean of 32.1 °C) in January 2013, which was the warmest month of the year, and cooled down in May 2013 with an average of 21 °C (BoM, 2017).

Twenty-week old *Eucalyptus tereticornis* seedlings in tube stock were chosen from a single local Cumberland plain cohort. Ten seedlings were harvested at the start of the experiment to measure initial leaf area and dry mass of foliage, woody components and roots. Forty-nine seedlings were used in the main experiment, allocated to seven treatments. The plants were grown in containers of differing volume set into the ground (5, 10, 15, 20, 25 or 35 L), or

were planted directly into soil (free seedlings, used as the control). All plants were grown in the open under field conditions, but were watered regularly to avoid moisture stress.

2.2 Experimental data acquisition

Full details of all measurements are given in Campany et al. (2017). The mass of each pool (foliage, wood, root, storage) was estimated over time as follows. The initial dry mass of leaves, woods and roots was measured for 10 seedlings at the start of the experiment using the harvesting procedure described in Campany et al. (2017). The dry mass of all experimental plants was measured at the end of the experiment following the same procedure. Seedling growth was tracked during the four months of the experiment, by measuring stem height (h), diameter at 15 cm height (d) and number of leaves on a weekly basis. These measurements were used to estimate the time course of wood and foliage biomass: for root total C we used only initial and final harvest measurements. Initial root C was estimated by averaging all 10 harvested seedlings.

We estimated weekly total C in wood ($C_{s,w}$) from the measurements of stem height and diameter, by using an allometric model fitted to initial and final harvest data.

$$\log\left(C_{t,w}\right) = b_1 + b_2 \log(d) + b_3 \log(h) \quad (1)$$

For each seedling, the total leaf area (LA) and foliage total C ($C_{t,f}$) over time (t) were estimated based on harvested data (T = time of harvest) and weekly leaf counts (LC) over time.

$$LA\ (t) = \frac{LA\ (T)}{LC\ (T)}\ LC\ (t) \quad (2)$$

$$C_{t,f}\ (t) = \frac{M_f\ (T)}{LC\ (T)}\ LC\ (t) \quad (3)$$

Fully expanded new leaves were sampled for total non-structural carbohydrate (NSC) concentration on a fortnightly basis. These concentrations were multiplied by leaf biomass to estimate the foliage TNC pool ($C_{n,f}$) at each time point. The partitioning of the non-structural C amongst foliage, wood and root tissues, according to empirically-determined fractions, was then used to estimate the wood and root components of the total TNC pool. Structural C mass for each component was estimated by subtracting non-structural C mass from total C mass.

Only foliage non-structural C ($C_{n,f}$) was measured, so to estimate the partitioning of the non-structural C among different organs, we used data from a different experiment on similar-sized seedlings of a related species (*Eucalyptus globulus*), which were grown in 5L pots until four months of age (Duan et al., 2013). We used data from the ambient well-watered control treatments. In that experiment, foliage, wood and root NSC were measured repeatedly over two months. There was no statistically significant change over time in the NSC distribution, so we used the mean distribution for mass-specific C_n over time, which was calculated to be a ratio of 75:16:9 among foliage, wood and root pools.

We estimated daily GPP from leaf-level gas exchange measurements and a simple canopy scaling scheme as described in Campany et al. (2017), and summarized below. Measurements of photosynthesis were made fortnightly throughout the experiment on one fully expanded leaf per plant (Campany et al., 2017). Photosynthetic CO_2 response (ACi) curves and leaf dark respiration rates (R) were measured on two occasions, 13-14th March 2013 (when new leaves were first produced) and 14-15th May 2013 (prior to the final harvest). The ACi curves were used to estimate photosynthetic parameters (the maximum rate of Rubisco carboxylation, V_{cmax} and the maximum rate of electron transport for RuBP regeneration under saturating light, J_{max}) using the biochemical model of Farquhar et al. (1980) and fit with the 'plantecophys' package (Duursma, 2015) in R. The parameter g_1, reflecting the sensitivity of stomatal conductance (g_s) to the photosynthetic rate, was estimated by fitting the optimal stomatal conductance model of Medlyn et al. (2011) to measured stomatal conductance data.

Treatment effects on photosynthesis were detected immediately on newly produced (fully expanded) leaves and Campany et al. (2017) did not observe variation over time in photosynthetic rates. Hence, the photosynthesis parameters were assumed not to change over time but were specific for each treatment. Therefore, daily net C assimilation per unit leaf area (C_{day}) was estimated by using a coupled photosynthesis–stomatal conductance model (Farquhar et al., 1980; Medlyn et al., 2011) using mean photosynthetic parameters (J_{max}, V_{cmax}, g_1 and R_d) for each treatment and meteorological data from the onsite weather station. The daily GPP was estimated by multiplying C_{day}, total leaf area (LA) and a self-shading factor. The self-shading factor, which is a linear function of LA, is calculated by via simulation with a detailed radiative transfer model, the 'YplantQMC' R package of Duursma (2014) for individual treatment. The leaf maintenance respiration rate (R_m, g C g^{-1} C plant d^{-1}) was calculated for each seedling by scaling the measured rate (R) to air temperature using a

Q_{10} value of 1.86 (Campany et al., 2017). The daily total maintenance respiration, $R_{m,tot}$ is calculated as a temperature-dependent respiration rate, R_m, multiplied by plant biomass. We assumed the same tissue-specific dark respiration rates for leaf, woody and root tissues for these seedlings, as was observed for seedlings of this species by Drake et al. (2017).

2.3 Carbon Balance Model (CBM)

We used a DA-modelling framework, similar to that used by Richardson et al. (2013). This approach uses a simple carbon balance model shown in Figure 1. The model is driven by daily input of gross primary production (GPP), which directly enters into a non-structural C pool (C_n). The daily total maintenance respiration, $R_{m,tot}$, is subtracted from C_n pool. The pool is then utilized for growth at a rate k (i.e. kC_n). Of the utilization flux, a fraction Y is used in growth respiration (R_g), and the remaining fraction (1-Y) is allocated to structural C pools (C_s): among foliage, wood and root ($C_{s,f}$, $C_{s,w}$, $C_{s,r}$). The foliage pool is assumed to turn over with rate s_f. We assume there is neither wood or root turnover as the seedlings in the experiment were young.

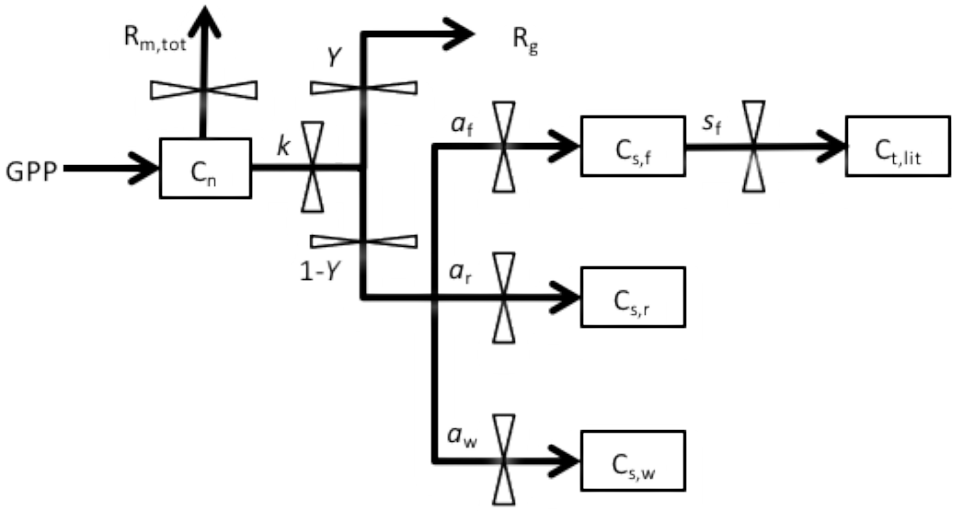

Figure 1: Structure of the Carbon Balance Model. Pools, shown as boxes: C_n, non-structural storage C; $C_{s,f}$, structural C in foliage; $C_{s,r}$, structural C in roots; $C_{s,w}$, structural C in wood. Fluxes, denoted by arrows, include: GPP, gross primary production; $R_{m,tot}$, total maintenance respiration; R_g, growth respiration; $C_{t,lit}$, structural C in leaf litterfall. Fluxes are governed by six key parameters: k, storage utilization coefficient; Y, growth respiration fraction; a_f, allocation to foliage; a_w, allocation to wood; a_r, allocation to roots; s_f, leaf turnover rate. a_r is defined as 1 - a_f - a_w.

The dynamics of the four carbon pools are described by four difference equations:

$$\Delta C_n = GPP - R_m\left(C_{t,f} + C_{t,w} + C_{t,r}\right) - k\,C_n \quad (4)$$

$$\Delta C_{s,f} = k\,C_n\,(1-Y)\,a_f - s_f\,C_{s,f} \quad (5)$$

$$\Delta C_{s,w} = k\,C_n\,(1-Y)\,a_w \quad (6)$$

$$\Delta C_{s,r} = k\,C_n\,(1-Y)\,a_r \quad (7)$$

Where GPP is the gross primary production (g C plant^{-1} d^{-1}); R_m is the maintenance respiration rate (g C g^{-1} C d^{-1}); $C_{t,f}$, $C_{t,w}$, and $C_{t,r}$ are the total C in foliage, wood and root respectively (g C plant^{-1}); k is the storage utilization coefficient (g C g^{-1} C d^{-1}); Y is the growth respiration fraction; a_f, a_w, a_r are the allocation to foliage, wood and root respectively; and s_f is the leaf turnover rate (g C g^{-1} C d^{-1}). a_r is defined as 1 - a_f - a_w.

The non-structural (storage) C pool (C_n) is assumed to be divided amongst foliage, wood and root tissues ($C_{n,f}$, $C_{n,w}$, $C_{n,r}$) according to an empirically-determined ratio of 75:16:9. Total carbon in each tissue (C_t) is then calculated as the sum of non-structural carbon (C_n) and structural carbon (C_s) for that tissue.

$$C_{t,f} = 0.75 \times C_n + C_{s,f} \quad (8)$$

$$C_{t,w} = 0.16 \times C_n + C_{s,w} \quad (9)$$

$$C_{t,r} = 0.09 \times C_n + C_{s,r} \quad (10)$$

2.4 Application of Data Assimilation (DA) algorithm

DA was used to estimate the six parameters (k, Y, a_f, a_w, a_r, s_f) of the CBM for this experiment. All parameters were allowed to vary quadratically with time, i.e. each parameter was represented as:

$$p = p_1 + p_2 t + p_3 t^2 \quad (4)$$

Quadratic variation over time was found to yield significantly better model fits than either constant parameter values or linear variation over time (see supplementary section S1). We executed three distinct sets of model simulations (Table 1), with the goals of (1) testing the need for a storage pool; (2) determining the effect of sink limitation on model parameters; and (3) attributing the overall effect of sink limitation on growth to the change in individual parameters.

For each set of model simulations, GPP and R_m were used as inputs to the DA framework, and the measurements of total C mass of each of the plant components and foliage NSC concentrations were used to constrain the parameter values. The set of constraints included 18 measurements of $C_{t,f}$ and $C_{t,w}$, two measurements of $C_{t,r}$ (start and end of the experiment), and six measurements of foliage NSC. There were 5 quadratically-varying parameters to determine for each treatment, summing to a total of 15 (3x5) coefficients to determine, compared with total 44 data measurements available, for each treatment.

We used the Metropolis algorithm (Metropolis et al., 1953) as implemented by Zobitz et al. (2011), with broad prior Probability Density Functions (PDFs) for the parameters (Table 2). Values of k, a_f, a_r and s_f were allowed to vary within the maximum possible range, while parameter Y was constrained according to the literature on growth respiration (Villar and Merino, 2001) . Parameter a_r was calculated from a_f and a_w with a check on a_r to ensure that it had reasonable values ($0 < a_r < 1$). Standard Error (SE) was used as an estimate of uncertainty on the assimilated data (Rowland et al., 2014; Richardson et al., 2010), and was calculated based on six replicate measurements. When combining errors, the errors were assumed to be uncorrelated (Hughes and Hase, 2010).

Model parameters were assumed to be real, positive and to have a lognormal probability distribution (Rowland et al., 2014). Therefore, all processes of parameter selection, and acceptance and rejection of parameters in relation to prior ranges were performed in lognormal space (Knorr and Kattge, 2005). We performed the first iteration starting from the prior set of parameters. To generate subsequent values for each parameter, a new point was generated by varying all vector elements by some step, chosen with a Gaussian distributed random number generator having a mean of 0 and a SD of 0.005 in log-normal space. We adjusted the step length for each parameter to values which lead to an average acceptance rate of the new points around 35–40%. We confirmed the chain convergence, having 3000 iterations to adequately explore the posterior parameter space, by visual inspection of the trace plots of different parameters as suggested by Van Oijen (2008). The trace plots show how the chain moves through parameter space for each individual parameter. The parameter vectors sampled during the first phase of the chain were not representative and therefore the first 10% of the chain was discarded from the posterior sample.

Table 1: Summary of the three model simulation sets

Simulation Set	Goal	Features	Addressing hypothesis
A	Test importance of storage pool	• DA applied to estimate parameters for model without storage pool and model with storage pool • Three treatment groups • Not constrained with NSC data • No leaf area feedback	H1
B	Identify effect of sink limitation on model parameters	• DA applied to estimate parameters for model with storage pool • Data divided into one, two, three or seven treatment groups • Constrained with NSC data • No leaf area feedback	H2-H5
C	Attribute overall effect on growth to changes in individual parameters	• Forward model runs to quantify impact of individual processes on overall plant growth • 5L and free seedlings treatments considered • Parameters changed individually and sequentially • Leaf area feedback on photosynthesis and R_m	

279 **Table 2:** Prior parameter PDFs (with uniform distribution) and the starting point of the
280 iteration for all parameters

Parameter	**Minimum**	**Maximum**	**Starting value**
k	0	1	0.5
Y	0.2	0.4	0.3
a_f	0	1	0.5
a_w	0	1	0.5
s_f	0	0.01	0.005
$a_r = 1 - (a_f + a_w)$, where $0 < a_r < 1$			

2.4.1 Importance of storage pool

We tested the hypothesis (H1) on the importance of including a non-structural C storage pool in CBM by contrasting fits of the full model with fits of a simplified model without the non-structural C pool (Simulation Set A, Table 1). The simplified model omits the non-structural C pool (C_s) from the full model (Figure 1) and assumes that all available C is utilized for growth each day. We applied the DA framework to both model options and calculated the Bayesian Information Criterion, BIC (Schwarz, 1978) to determine the better model structure. BIC measures how well the model predicts the data based on a likelihood function and compare model performance taking into account the number of fitted parameters, with the lowest BIC number indicating the best model setting. For this comparison, both models were fit to the biomass data only, not leaf NSC data, in order to ensure that both models were fit to the same number of data points.

2.4.2 Effects of sink limitation on model parameters

The effects of sink limitation on C balance were investigated by applying the DA framework to data from all treatments combined, and then subsets of treatments (Simulation Set B, Table 1). Considering all treatments pooled together gives same parameters for all the treatments and effectively assumes no effect of sink limitation. On the other hand, taking more subsets of treatments produces more parameter sets (one for each subset) and allows for parameters to vary according to the degree of sink limitation. We first fitted the model to all data, ignoring treatment differences; then considered 2 treatment groups (free seedling / 5-35 L containerized seedlings), 3 groups (free / 5–15 L / 20–35 L) and 4 groups (free / 5-10 L / 15-20 L / 25-35 L). We also fitted the model to each of the 7 treatments individually, where the parameter set for each treatment is unique. The BIC values were compared across treatment groupings.

2.4.3 Attribution analysis

We performed a sensitivity analysis to quantify the impact of the response of each individual process to sink limitation on overall plant growth (Simulation Set C, Table 1). This analysis consisted of forward runs of the model, including a leaf area feedback to GPP. That is, rather than taking GPP based on measured LA (Eq. 9) as input, in this version of the model we calculated daily GPP using the modelled LA, the photosynthesis rate and corresponding self-shading factor. Adding the LA feedback to the model was necessary to quantify how the treatment effect on individual model parameters affects final seedling biomass through its effect on foliage mass, and consequently GPP, over time.

LA in each time step is estimated from NSC-free specific leaf area (SLA_{nonsc}) and the predicted foliage structural carbon ($C_{s,f}$) in that time step. SLA_{nonsc} is calculated at harvest discarding the foliage NSC portion and is assumed to be constant for a given treatment throughout the experiment.

$$LA = SLA_{nonsc} \times C_{s,f} \quad (12)$$

Once the LA feedback was implemented in the CBM, we ran the model with the inputs and modelled parameters from the smallest pot seedling (5 L), then changed the parameters to those for the free seedling sequentially in order to quantify the effect of each parameter on the final seedling biomass. The parameters we considered for this attribution analysis were: daily photosynthetic rate per unit leaf area (C_{day}), maintenance respiration rate (R_m), C allocation fractions to biomass (a_f, a_w, a_r), growth respiration rate (Y), foliage turnover rate (s_f) and utilization coefficient (k). We additionally carried out a sensitivity analysis in which we varied each parameter from its baseline value separately.

326

327 # 3 Results

328 ## 3.1 Importance of storage pool

329 First, we tested the null hypothesis (H1) that there is no need for a non-structural
330 carbohydrate storage pool in the carbon balance model. We compared BIC values for model
331 structures with and without a storage pool. Table 3 (Simulation Set A) shows the results for
332 model fits with the optimal grouping strategy (three treatment groups). BIC values were
333 consistently lower for the model including the storage pool; the improvement in model fit is
334 most noticeable for the containerized seedlings. This analysis demonstrates that the model
335 does need to include a storage pool to correctly represent the experimental data. In all
336 remaining analyses, the full CBM (with non-structural C pool) is applied to data from all four
337 plant C pools (NSC, foliage, wood and root biomass).

338 **Table 3:** BIC values from model fits. The lowest BIC values indicate the best performing
339 parameter settings for any particular simulation. Note that, for Sim A, leaf NSC data were not
340 used to constrain either model, to ensure that both models were fit to the same dataset,
341 resulting in lower BICs compared to Sim B. Treatment groups are: 'Small' - 5 L, 10 L and 15
342 L containers; 'Large' - 20 L, 25 L and 25 L containers; 'Free' – freely rooted seedlings; 'All'
343 - all data; 'Containerized' - all plants in containers.

Simulation Set	Model Setting	Treatment groups	BIC
Sim A	Model without storage pool	Small	459
		Large	550
		Free	182
	Model with storage pool	Small	215
		Large	338
		Free	167
Sim B	7 treatments combined	All	2768
	2 groups	Containerized	1813
		Free	170
		Total	1983
	3 groups	Small	683
		Large	457
		free	170
		Total	1310
	7 treatments individually	5 L	85

		10 L	98
		15 L	60
		20 L	63
		25 L	106
		35 L	152
		Free	170
		Total	734

3.2 Sink limitation effect on C balance processes

We addressed our second null hypothesis (H2), that there is no effect of sink limitation on carbon balance processes, by comparing BIC values obtained for model fits when all treatments were combined vs separating the treatments into sub-groups. If there was no effect of sink limitation, the BIC value when all treatments are fit together would be similar to that obtained when treatments are separated into groups. The BIC values shown in Table 3 (Simulation Set B) decrease strongly as number of treatment groups increases, indicating a clear effect of sink limitation on carbon balance processes. Although the BIC values continue to decrease as more treatment groups are considered, we also found that interpreting parameter changes became more difficult as the number of groups increased. Hence, further analyses in this paper used unique parameter sets for three treatment groups: small containers, large containers, and free seedlings.

3.3 Analysis of carbon stock dynamics

Figure 2 shows the correspondence between modeled C pools and data. The model reproduced the key features of biomass growth over time in response to treatment. Biomass growth (Figure 2A, B and C) and the foliage storage pool (Figure 2D) were very clearly impacted by sink limitation: biomass growth was strongly reduced for containerised seedlings, which was very well mimicked by the model. Foliage growth in the free seedlings slowed towards the end of the experiment. Wood and root growth continued throughout the experiment in freely-rooted seedlings but slowed down during the second half of the experiment in containerized seedlings. NSC concentrations ($C_{n,f}$ / $C_{t,f}$) in seedlings in small containers were higher compared those in free seedlings at the beginning of the season but all treatments had similar concentrations after four months (Figure 2D). In March, at the time of the first leaf NSC measurements, the foliage storage pool (Supplementary Figure S1) was similar in size across all treatments, but it increased over time in the free seedlings as these plants continued to grow, and decreased over time in the plants in small containers.

Modelled C stocks for all 7 treatments closely tracked their corresponding observations (Figure 2) as most of the predicted biomass values were within one standard error of the measurements. The exception is the 35 L container treatment, which is underestimated slightly because the grouping of 20, 25 and 35 L treatments into one group makes it difficult for the model to fit all treatments in this group.

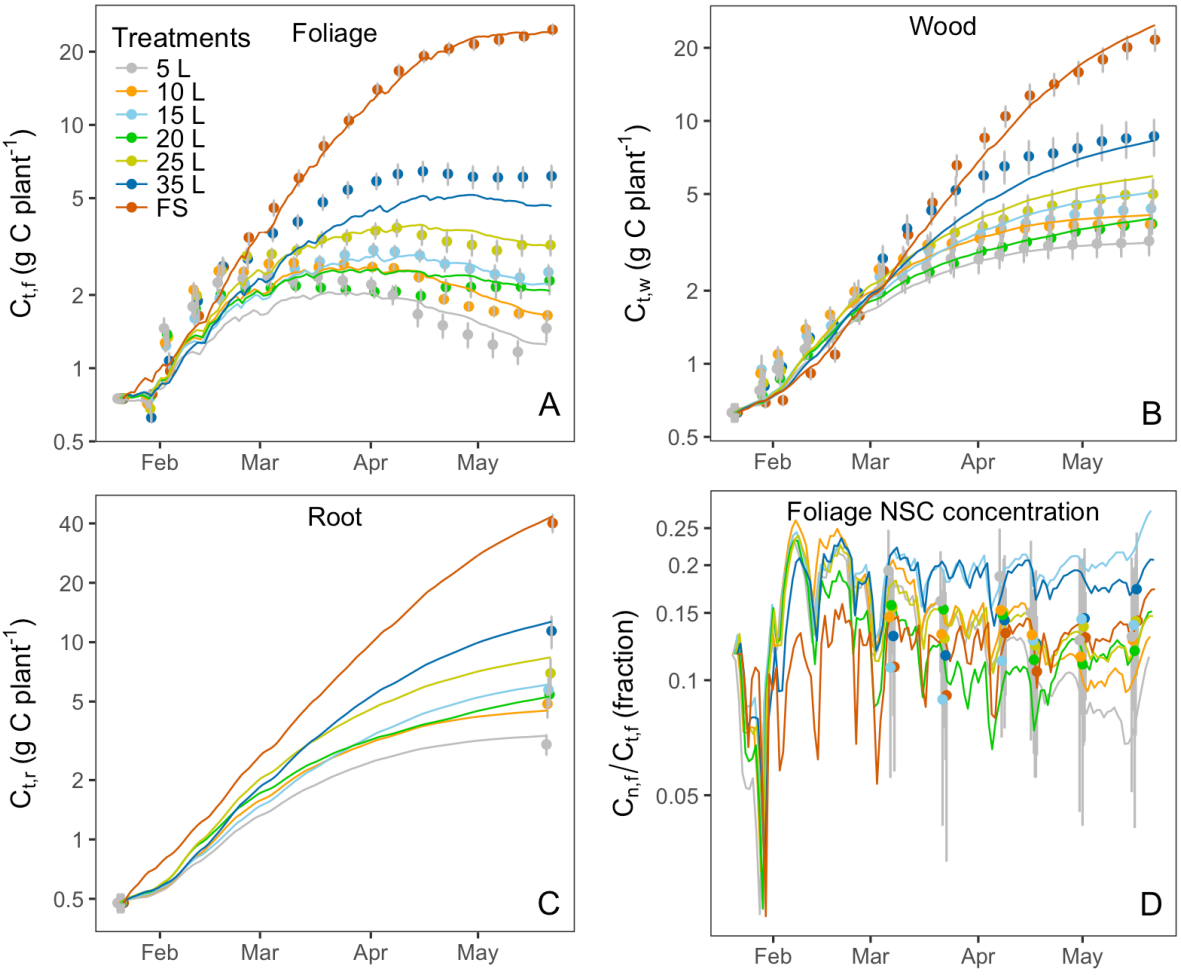

Figure 2: C stocks (lines) with the inferred parameter set and corresponding observations (symbols): (A) total C mass in foliage $C_{t,f}$, (B) total C mass in wood $C_{t,w}$, (C) total C mass in root $C_{t,r}$ and (D) foliage NSC concentration ($C_{n,f}/C_{t,f}$). Note that the carbon pools and foliage NSC concentration (y-axes) are plotted on log scale to visualize the changes at the beginning of the experiment. Error bars (1 SE, n = 6) are shown for each observation.

381

382 **3.4 Parameter estimates**

383 Data assimilation indicated significant treatment effects on all five fitted parameters (Figure
384 3). There was a large effect of sink limitation on the utilization coefficient (k). In agreement
385 with our hypothesis H3, the free seedling had the highest k, and the seedlings in small
386 containers (most sink limited) had the lowest k (Figure 3A). As the experiment progressed,
387 the utilization rate of free seedlings began to decrease (Figure 3A). In contrast to the free
388 seedlings, the potted seedlings had relatively low utilization rates initially (k close to 0.5) and
389 the utilization rates slowed down abruptly with time, most significantly in the smallest
390 container treatments (Figure 3A).

391 In agreement with hypothesis H4, the estimated growth respiration rate (Y) varied according
392 to the sink strength of the treatment groups, and was highest in the lowest sink strength
393 treatments (Figure 3B). Moreover, Y did not vary significantly over time for the sink limited
394 treatment groups. However, the rate of growth respiration for the free seedling slowed down
395 over time.

396 The data assimilation process also indicated that the growth allocation fractions vary among
397 treatments and over time. Consistent with hypothesis H5, wood allocation fraction was
398 highest in the smallest container treatments, and lowest in the free seedlings (Figure 3D). For
399 the free seedlings, allocation was initially highest to foliage and roots (Figure 3C-E); over
400 time, the plants reduced allocation to foliage and increased it to wood and roots. In the
401 containerized seedlings, allocation was initially highest to wood and foliage; over time,
402 foliage allocation decreased to almost zero and root allocation increased.

403 The estimated leaf turnover rate, s_f was also notably higher for sink-limited treatments
404 compared to free seedlings (Figure 3F). The large value of modelled leaf litterfall for sink-
405 limited treatments is consistent with observations during the experiment that containerized
406 seedlings had relatively large leaf litterfall, beyond normal senescence. Estimated s_f increased
407 over time for all treatment groups (most notably in free seedlings), due to a combination of
408 ontogeny, seasonal change, and growth restriction in the sink-limited seedlings.

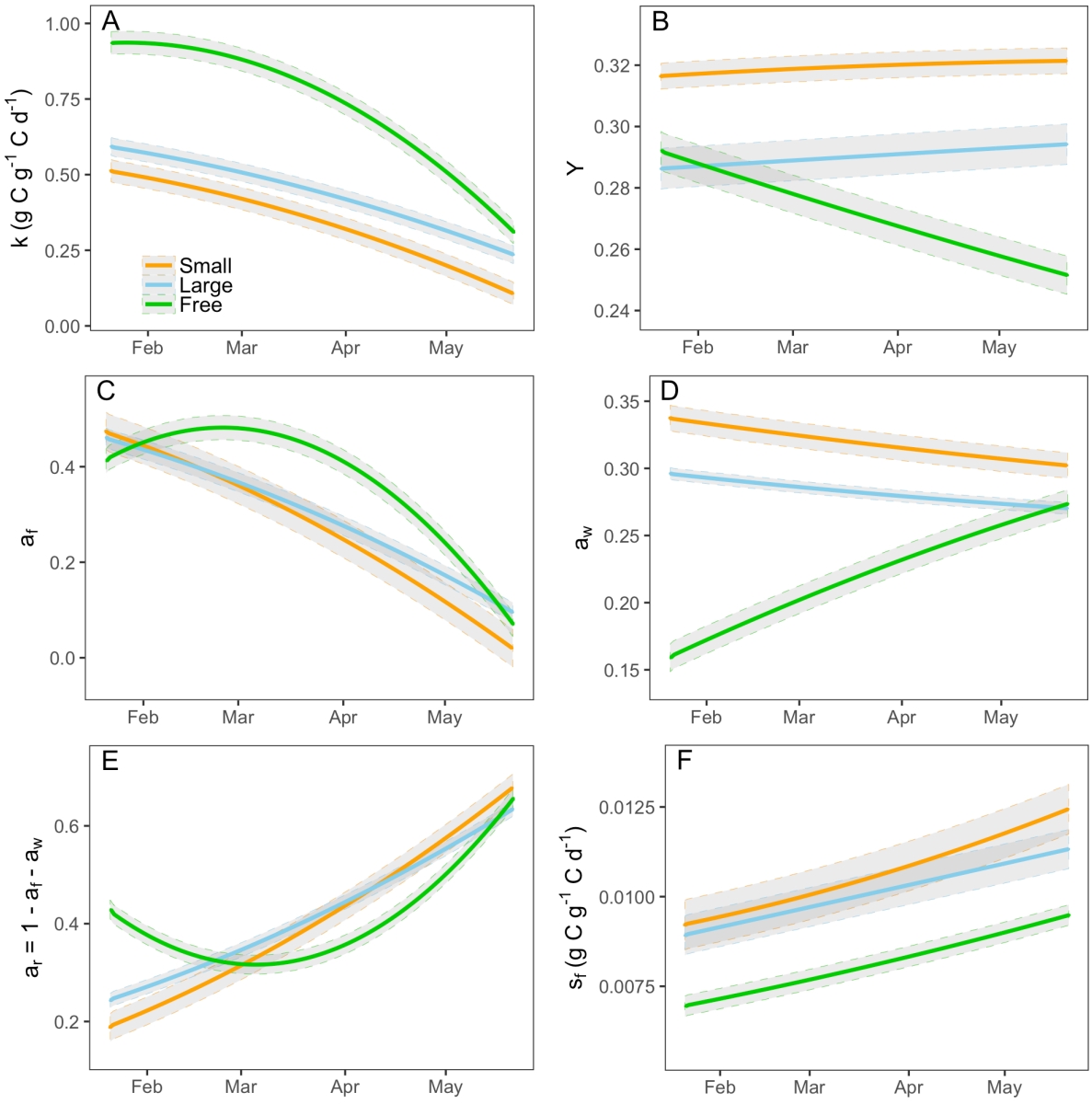

409

410 **Figure 3**: Modelled final parameters for three groups of treatments during the experiment
411 period (21st Jan to 21st May 2013): (A) storage utilization coefficient, k; (B) growth
412 respiration fraction, Y; (C) allocation to foliage, a_f; (D) allocation to wood, a_w; (E) allocation
413 to roots, a_r and (F) leaf turnover rate, s_f. a_r is defined as 1 - a_f - a_w. The grey shaded area
414 shows the 95% confidence intervals of modelled parameters.

415

416 **3.5 Carbon budget**

417 The model was used to partition total GPP (g C plant^{-1}) from the entire experiment period
418 into different C pools (growth respiration, maintenance respiration, non-structural carbon,
419 structural foliage, wood, and root carbon, and litterfall) for all 7 treatments (Figure 4). Total

GPP was considerably lower for the containerized seedlings, owing to lower photosynthetic rates per unit leaf area, C_{day} (Figure 5A), and lower total leaf area (LA) per plant. Though starting with the same total LA of 0.016 m^2, the 5 L containerized and free seedlings had total LA of 0.031 and 0.516 m^2 respectively after four months of treatment. Simultaneously, the partitioning of GPP changed considerably across different treatments.

Small container seedlings (5, 10, 15 L) had a higher fraction of GPP lost in leaf litterfall compared to other seedlings (Figure 4), consistent with observations during the experiment. The proportion of GPP in final foliage mass was extremely low in sink limited treatments (also shown in Figure 2A). Allocation of GPP to final foliage and root biomass were highest in the free seedlings, although interestingly allocation to final wood biomass was similar across treatments. The final allocation to storage was also higher in free seedlings. The sink limited seedlings had a higher proportional C lost through maintenance respiration. Tissue specific respiration rates were similar in free and containerized seedlings, so the ~35% reduction in photosynthetic rate for the smallest containerized seedling, led to a higher overall $R_{m.tot}$/GPP fraction. In summary, the estimated total respiration ($R_{m.tot} + R_g$) to GPP ratio was considerably lower for the free seedlings compared to the sink limited treatments. The carbon use efficiency (CUE) remained relatively constant and high over time for free seedlings (~0.65), whereas CUE in the smallest container treatments showed a sharp reduction over time down to ~0.25 (Supplementary Figure S2).

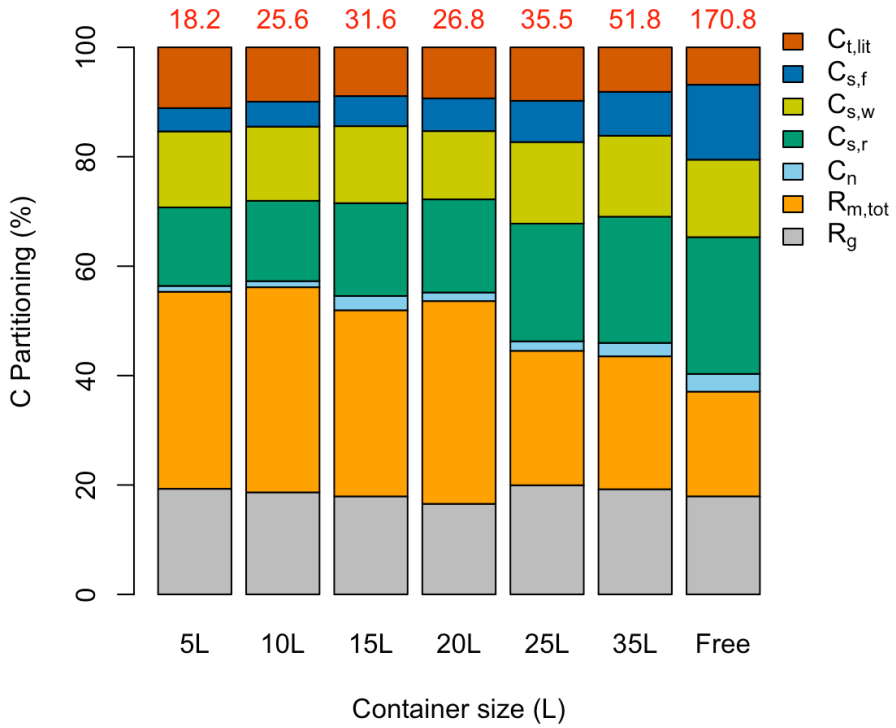

439

440 **Figure 4:** Simulated proportional C partitioning for the whole experimental period. The total
441 accumulated GPP (g C plant^{-1}) for individual treatments is shown (in red) at the top of each
442 column. Free stands for free seedling. Different C partitions are in the colour legend: total
443 litterfall, $C_{t,lit}$; foliage structural C, $C_{s,f}$, wood structural C, $C_{s,w}$, root structural C, $C_{s,r}$; non-
444 structural C pool, C_n; total maintenance respiration, $R_{m,tot}$ and growth respiration, R_g.

445

446 **3.6 Attribution analysis**

447 Sink limitation affected biomass growth via a range of processes, namely reduction in
448 photosynthesis, and variation in the utilization rate, growth respiration, leaf litterfall, and C
449 allocations to foliage, wood and root across various treatment groups. We quantified the
450 contribution of each of these process responses separately by running the CBM with
451 parameter inputs changing both sequentially and individually (one at a time). Table 4 presents
452 the effect of the parameters changing individually from the value of the smallest container
453 treatment (5 L) to that of free seedling (FS) and other way around, resetting the previous
454 parameter to the baseline value. The final biomass values in Table 4 indicate the contribution
455 of each individual parameter separately and sequentially. Photosynthetic capacity had the
456 largest individual effect on total plant growth (+15.28 and -71.9 g C) compared to the rest of

457 the parameters. However, allocation pattern and the utilization rate also had a sizeable effect
458 on final biomass (Table 4).

459 Figure 5 shows how biomass (M_f, M_w and M_r) is predicted to change when each parameter is
460 changed sequentially from the parameter set derived from DA on the 5L observations (gray
461 line, Figure 5) to that of the parameters obtained when using the free seedlings as constraint
462 of the model (red line, Figure 5). Daily net C assimilation per unit leaf area (C_{day}), which was
463 30% higher for free seedling compared to 5 L container treatment (Figure 5A), had a large
464 impact on plant growth (final total biomass was increased by 11 g, Table 4 and Figure 5G-I,
465 gray to orange). Maintenance respiration rate (R_m) did not vary significantly across
466 treatments (Figure 5B), in line with the data presented in Campany et al. (2017), and
467 consequently its impact was insignificant (the final total biomass is reduced by only 0.24 g,
468 Table 4 and Figure 5G-I, orange to light blue). The modelled biomass allocation fractions (a_f,
469 a_w and a_r) in Figure 5C had important, but mixed, effects on C stocks. The final foliage mass
470 was increased from 3.4 g to 9.6 g due to the increase in C allocation to foliage (Figure 5G,
471 light blue to green), which has a positive feedback on GPP. Concomitant changes in C
472 allocation to wood and root resulted in smaller changes to these biomasses as shown in
473 Figure 5H-I (2.5 g and 7.0 g rise respectively). Overall, the change in allocation pattern
474 resulted in an increase in final total biomass by 15.74 g (Table 4). Growth respiration rate (Y)
475 was ~20% lower in free seedlings (Figure 5D), which had a considerable impact on C
476 budgets (the final total biomasses were increased by 9.56 g, Table 4 and green to yellow,
477 Figure 5G-I). Leaf turnover, s_f was low in the free seedlings compared to the 5 L container
478 treatment (Figure 5E) which had a large positive effect on final C pools (Figure 5G-I, yellow
479 to blue). The foliage mass was increased by 5.6 g; the wood and root masses were also
480 further increased (3.4 g and 5.8 g respectively) due to the increase in GPP when foliage is
481 retained for longer. Finally, the utilization coefficient, k was higher in free seedlings (Figure
482 5F) causing a 20-30% positive feedback on C budgets (total biomass increased by 23.08 g,
483 Table 4 and Figure 5G-I, blue to red).

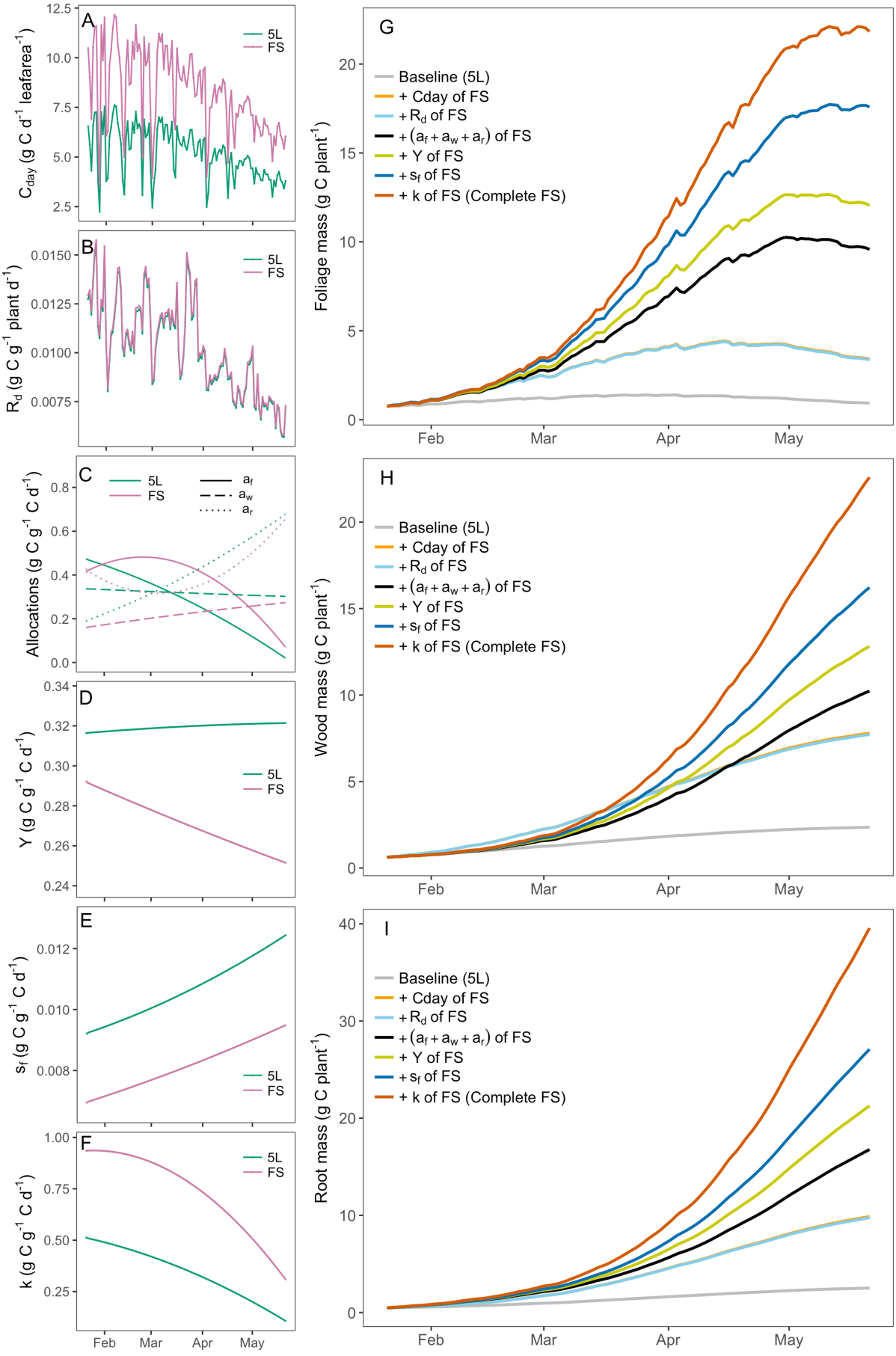
A
B
C
D
E
F
G
H
I
5L
FS
Baseline (5L)
+ Cday of FS
+ Rd of FS
+ (af + aw + ar) of FS
+ Y of FS
+ sf of FS
+ k of FS (Complete FS)
af
aw
ar
Cday (g C d-1 leafarea-1)
Rd (g C g-1 plant d-1)
Allocations (g C g-1 C d-1)
Y (g C g-1 C d-1)
sf (g C g-1 C d-1)
k (g C g-1 C d-1)
Foliage mass (g C plant-1)
Wood mass (g C plant-1)
Root mass (g C plant-1)
Feb
Mar
Apr
May

484

Figure 5: Attribution analysis. Left column (A-F): changes in inferred parameters; Right column (G-I): associated impacts on C budgets due to sequential parameter changes from 5 L container treatment to that of free seedling (right column, G-I). Different colours in the figure indicate the parameter shifts (left column, A-F) and their associated impacts on C budgets (right column, G-I). Legend: 5L, highly sink-limited treatment with container size of 5 L; FS, Free Seedling without any sink limitation. Note that the orange line is overlain by the light blue line: the small change in maintenance respiration results in a very minor effect on biomass growth.

Table 4: Estimates of final biomass due to parameter change (individual and sequential), showing the contribution of each parameter separately and successively to biomass changes. All values in g C plant^{-1}. +/- indicates biomass increase or decrease due to particular parameter change. The final column corresponds to the changes shown in Figure 5.

Parameter change	Individually		Sequentially
	5 L » FS	FS » 5 L	5 L » FS
Baseline C_t	5.81	83.99	5.81
C_{day}	+15.28	-71.9	+15.28
R_d	-0.08	+1.1	-0.24
$(a_f + a_w + a_r)$	+1.53	-45.5	+15.74
Y	+0.41	-19.22	+9.56
s_f	+1.13	-19.17	+14.77
k	+0.44	-23.08	+23.08
		FS total observed C_t	83.99

4 Discussion

4.1 Effects of sink limitation on C balance

Our DA-model analysis of this root volume restriction experiment provided significant new insights in the response of key C balance processes to sink limitation. We were able to infer that, in addition to a reduction in photosynthetic rates, sink limitation reduced NSC utilization rates, increased growth respiration, modified allocation patterns and enhanced senescence. Our attribution analysis indicated that all of these process responses contributed significantly to the overall reduction in biomass observed under low rooting volume.

We first tested the null hypothesis (H1) that seedling growth rates could be adequately predicted from current-day photosynthate. This hypothesis was rejected, with a storage pool being necessary to simulate growth, particularly for containerized seedlings (Sim A, Table 3). The approach of simulating growth from current-day photosynthate is commonly used in models, particularly for evergreen plants (e.g. (Jain and Yang, 2005; Law et al., 2006; Thornton et al., 2007)), but several authors have proposed the need for a storage pool to balance the C sources and sinks in the short term, as well as simulate the effects of photosynthetic down-regulation in the long-term (Pugh et al., 2016; Richardson et al., 2013; Fatichi et al., 2016). Our results support the need for an NSC pool in CBMs.

We then tested the second null hypothesis (H2) that there was no effect of treatment on the parameters of the C balance model. This hypothesis was also rejected: fitting the DA-model framework simultaneously to all treatments with one set of parameters (ignoring sink limitation effect) gave a low goodness of fit (Sim B, Table 1). This result is consistent with the finding of Campany et al. (2017) that the observed effects of sink limitation on photosynthesis in this experiment were insufficient to explain the large reduction in biomass. Instantaneous photosynthetic rates were reduced 20-30% by sink limitation. Our DA analysis indicated that several other processes contributed to the reduction in biomass growth, including carbohydrate utilization, growth respiration, allocation patterns, and turnover.

Our results suggested a significant effect of sink limitation on the carbohydrate utilization rate, k (Figure 3A). The modelled k values were approximately twice as large in free seedlings compared to the small containers. This result supports the hypothesis (H3) that plants would have the lowest utilization rate under sink-limited conditions. At the start of the measurement period, the free seedlings were utilizing almost all C produced immediately in growth (k close to 1.0, Figure 3A). The utilization coefficient of the free seedlings decreased over time, causing a build-up in C storage (Figure 2D). This decrease in utilization rate could potentially be an ontogenetic effect, with free seedlings initially allocating all carbon to growth during establishment but increasing storage with increasing size. However, ontogenetic effects are confounded with season in this experiment, such that decreasing utilization rates over time could also be a result of decreasing temperatures moving into autumn. There is a real need to quantify how the carbohydrate utilization rate varies with environmental conditions and ontogeny; data assimilation of experiments in which photosynthesis and growth rates have been monitored over time offer one means to do so.

Although the carbohydrate utilization rate was highest in the free seedlings, leaf carbohydrate concentrations were not lower in these plants at the end of the experiment. As shown in the final C budget analysis (Figure 4), there was a higher total C allocation to the NSC pool in free seedlings than sink-limited treatments. Final carbohydrate storage was high in free seedlings despite high k because the carbohydrate pool was recharged throughout the experiment (Figure 2D), as the free seedlings had high photosynthetic rates but no higher maintenance respiration requirement. In contrast, NSC was depleted for the smallest pot treatments after mid-March (Figure 2D) when demand exceeded supply due to both limited production of photoassimilates and enhanced leaf litterfall (Figure 3F).

The modelled rate for growth respiration, Y was larger for sink limited treatments than the free seedling (Figure 3B). Overall, there was lower C utilization (i.e. CUE) in plant structural growth in sink-limited treatments (~45%) compared to free seedlings (~60%). This finding supports the "wasteful plant" hypothesis H4. Inferred Y remained constant over time for the containerized treatments, implying a fixed portion of C loss due to growth respiration despite seasonal variation. However, a reduction in Y over time was inferred for the free seedling, suggesting a possible ontogenetic effect. However, it is important to note that we have inferred growth respiration from the CBM framework. Therefore, these estimates could possibly also include C losses via other pathways. Direct measurements of growth respiration rates would be useful to confirm the inferred effects of sink limitation and investigate potential underlying mechanisms.

We also demonstrated that the allocation fractions among organs change in sink-limited conditions, with sizeable consequences for plant growth rates. Previous analyses of pot-size experiments have generally only been able to estimate changes in final biomass partitioning (e.g. Poorter et al. 2012a). Campany et al. (2017) analysed final biomass partitioning in the experiment and did not find any significant difference in biomass partitioning in sink-limited seedlings compared to free seedlings, once ontogenetic drift was taken into account. Our analysis adds to that of Campany et al. (2017) by calculating the dynamics of allocation over time and taking estimated foliage loss into account. Our analysis showed that modelled allocation fractions vary significantly over time (Figure 3C, D and E). In the free seedlings, allocation to foliage decreased, and allocation to both wood and roots increased, reflecting the ontogenetic effects mentioned by Campany et al. (2017). However, our analysis also highlights significant variations among treatments in the modelled C allocation fractions to

foliage, wood and root that are not ontogenetic. At the beginning of the experiment, foliage allocation fractions were similar for all treatment groups, but wood allocation was higher, and root allocation lower, in the containerized seedlings compared to the free seedlings. For the containerized seedlings, changes over time also differed from those in the free seedlings: wood allocation decreased marginally, rather than increasing, foliage allocation declined steeply over time, and root allocation increased steeply. These allocation patterns in seedlings supported our hypothesis H5 that sink limitation due to root restriction would favour allocation to wood over foliage or fine roots. Calculating dynamic allocation patterns over the course of an experiment thus provides additional insights beyond analysis of the final biomass outcome.

4.2 Application of DA to infer C balance processes

We have demonstrated that the DA approach can be an invaluable tool for quantifying C fluxes in experimental systems, enabling us to extract important new information from existing datasets to inform carbon balance models, such as the rate and timing of the transfer of photosynthate to and from storage pools. The DA-modelling approach is able to draw together the experimental data to estimate all the components of C balance, including photosynthesis, respiration, NSC, biomass partitioning and turnover. This approach could readily be applied to other experiments to derive new information allowing better representation of C balance processes in vegetation models.

Applying this approach requires a range of measurements to constrain the key C balance processes. Here, we used estimated daily C assimilation and maintenance respiration rate as model inputs and constrained the model with measurements of biomass pools (foliage, wood, root) and foliage NSC concentrations. We used fortnightly foliage and wood biomass measurements; the DA framework would work with fewer data observations, but parameters would be estimated with less accuracy. Informal exploration of the model suggested that measurements of foliage turnover would have been particularly useful to better constrain the model. Any experiment having estimates of GPP, maintenance respiration, and structural biomass could potentially be investigated with this framework. However, additional measurements of storage and turnover would be highly beneficial for the performance of the simulation. Repeated observations over time are also useful, particularly for young plants, to account for variations in parameter values over time. We found significant changes in

parameter values during the course of the 4-month experiment, which may be linked to both ontogeny and seasonal variation in temperature.

One major caveat on our results is that below-ground carbon cycling processes were not well characterized. For practical reasons, processes such as root growth, respiration, turnover, and exudation are rarely well quantified in empirical studies. Here, we had access to initial and final estimates of root biomass. Root respiration was estimated; root turnover and exudation were assumed to be zero. There is evidence that stress can increase rates of root exudation: for example, Karst et al. (2016) demonstrate increased exudation rates in seedlings exposed to cold soils. They also showed that stressed plants may exude C beyond that predicted by simple concentration gradients in NSC between root and soil. The loss of C independent of NSC in roots suggests that exudation may be actively enhanced once plant growth is limited (Hamilton et al., 2008; Karst et al., 2017). As our CBM does not include this process, it would attribute any C loss through root exudation to another process removing C from the plant, such as growth respiration. The increase in growth respiration that we inferred may thus potentially include root exudation. We have reasonable confidence, from the combination of measurements available, in our inference that the C loss term was increased with sink limitation. However, direct measurements of one or both processes would be required to determine the role of root exudation.

In addition, we did not have access to estimates of root or wood NSC. We used data measured in a previous experiment on 4-month old *E. globulus* seedlings (Duan et al. 2013) to estimate these values from foliage NSC. It would have been useful to obtain these values, particularly since wood and root tissue can act as storage organs, and the timing of storage development would be extremely useful to quantify. The concentration of NSC in plant roots measured by Duan et al. (2013) was relatively small compared to that of foliage (mean 2.15%). However, fine root NSC values in a nearby experiment on 17-month-old *E. parramattensis* saplings were even lower (0.78%) (Morgan E. Furze et al. unpublished data). It is possible that these very fast-growing Eucalypt species only start to accumulate root reserves when they are established. Further research is needed to quantify the trade-off between allocation to growth and storage during establishment.

4.3 Implications for modelling plant growth under sink limited conditions

The goal of our study was to examine how carbon balance models should be modified to represent sink limitation of growth, whilst maintaining mass balance. Our results demonstrate that several process representations need to be modified. Firstly, we demonstrate a clear need to incorporate a carbohydrate storage pool, with a dynamic utilization rate for growth. We demonstrate that the utilization rate is slowed by sink limitation, and may also vary with ontogeny. Targeted experimental work is needed to better quantify this variation in utilization rates. Secondly, in addition to a feedback on photosynthetic rates, other plant processes including growth respiration, turnover and allocation are also affected by sink limitation. Applying a DA-modelling framework to experimental data with rooting volume restriction has allowed us to quantify these effects in this experiment. Applying this approach more broadly would potentially allow us to identify general patterns that could then be formulated for inclusion into models.

The inferences on carbohydrate dynamics from seedling studies could be used to infer mature tree responses that can subsequently be integrated at ecosystem level and beyond using the concepts of Hartmann et al. (2018). We are enthusiastic to see the approach applied to other experiments, but there are likely to be gaps in the datasets to constrain the key C balance processes. Fortunately, the DA approach does not require continuous measurements of all of the C stocks and fluxes. In the absence of measurements, the model can be relied upon to project the time evolution of missing stocks and fluxes, although of course, the precision of model estimates and insights that can be gained, increases with data availability. DA can also be applied at ecosystem scale. There are several successful examples of DA being applied to forest growth, albeit without a focus on storage (e.g. Van Oijen (2008); Williams et al. (2005); Bloom et al. (2016); Quaife et al. (2008); Pinnington et al. (2016)). Overall, this approach provides important insights into the regulation of carbohydrate storage and would significantly advance our ability to predict the impacts of environmental changes on plant growth and vulnerability to stress.

Data availability

The raw data are freely available on Figshare (doi: https://doi.org/10.6084/m9.figshare.5125087.v3). The R source code to perform all the data processing and analysis to replicate the figures is freely available as a Git repository (https://github.com/kashifmahmud/DA_Sink_limited_experiment).

663

664 **Author contribution**

665 KM analyzed the data, developed the model code, performed the simulations and wrote the
666 paper. BEM conceived the idea and helped in data analysis. RAD and CC provided the
667 experimental data. BEM, RAD, CC and MGD provided in-depth editing of the manuscript.

668

669 **Competing interests**

670 The authors declare that they have no conflict of interest.

671

672 **Acknowledgements**

673 This research was supported by the Australian Research Council (Discovery, DP
674 DP160103436), the Hawkesbury Institute for the Environment, and Western Sydney
675 University. The authors wish to thank Burhan Amiji for his technical assistance and all
676 individuals from Hawkesbury Institute for the Environment who helped during the
677 experimental harvest. We thank Mathew Williams for advice on implementing the data
678 assimilation framework.

679

680 **References**

681 Arp, W. J.: Effects of source sink relations on photosynthetic acclimation to elevated carbon
682 dioxide, Plant, Cell and Environment, 14, 869-876, 1991.

683 Bloom, A. A., Exbrayat, J.-F., van der Velde, I. R., Feng, L., and Williams, M.: The decadal
684 state of the terrestrial carbon cycle: Global retrievals of terrestrial carbon allocation, pools,
685 and residence times, Proceedings of the National Academy of Sciences, 113, 1285-1290,
686 10.1073/pnas.1515160113, 2016.

687 BoM: Climate Data Online (Station 067105), Bureau of Meteorology Melbourne.
688 http://www.bom.gov.au/climate/data/ (Accessed 26-08-2017). 2017.

689 Bossel, H.: treedyn3 forest simulation model, Ecol. Model., 90, 187-227,
690 https://doi.org/10.1016/0304-3800(95)00139-5, 1996.

691 Bradford, K. J., and Hsiao, T. C.: Stomatal behavior and water relations of waterlogged
692 tomato plants, Plant Physiol, 70, 1508-1513, 1982.

693 Buckley, T. N.: The control of stomata by water balance, New Phytologist, 168, 275-292,
694 10.1111/j.1469-8137.2005.01543.x, 2005.

695 Campany, C. E., Medlyn, B. E., and Duursma, R. A.: Reduced growth due to belowground
696 sink limitation is not fully explained by reduced photosynthesis, Tree Physiol, 37, 1042-1054,
697 10.1093/treephys/tpx038, 2017.

698 Crous, K. Y., and Ellsworth, D. S.: Canopy position affects photosynthetic adjustments to
699 long-term elevated CO2 concentration (FACE) in aging needles in a mature Pinus taeda
700 forest, Tree Physiol, 24, 961-970, 2004.

701 De Kauwe, M. G., Medlyn, B. E., Zaehle, S., Walker, A. P., Dietze, M. C., Wang, Y. P., Luo,
702 Y. Q., Jain, A. K., El-Masri, B., Hickler, T., Warlind, D., Weng, E. S., Parton, W. J.,
703 Thornton, P. E., Wang, S. S., Prentice, I. C., Asao, S., Smith, B., McCarthy, H. R., Iversen,
704 C. M., Hanson, P. J., Warren, J. M., Oren, R., and Norby, R. J.: Where does the carbon go? A
705 model-data intercomparison of vegetation carbon allocation and turnover processes at two
706 temperate forest free-air CO2 enrichment sites, New Phytologist, 203, 883-899,
707 10.1111/nph.12847, 2014.

708 de Wit, C. T.: Simulation of assimilation, respiration, and transpiration of crops, Wiley, 1978.

709 de Wit, C. T., and van Keulen, H.: Modelling production of field crops and its requirements,
710 Geoderma, 40, 253-265, https://doi.org/10.1016/0016-7061(87)90036-X, 1987.

711 Drake, J. E., Vårhammar, A., Kumarathunge, D., Medlyn, B. E., Pfautsch, S., Reich, P. B.,
712 Tissue, D. T., Ghannoum, O., and Tjoelker, M. G.: A common thermal niche among
713 geographically diverse populations of the widely distributed tree species Eucalyptus
714 tereticornis: No evidence for adaptation to climate-of-origin, Glob. Change Biol., 23, 5069-
715 5082, doi:10.1111/gcb.13771, 2017.

716 Duan, H., Amthor, J. S., Duursma, R. A., O'Grady, A. P., Choat, B., and Tissue, D. T.:
717 Carbon dynamics of eucalypt seedlings exposed to progressive drought in elevated [CO2] and
718 elevated temperature, Tree Physiol., 33, 779-792, 10.1093/treephys/tpt061, 2013.

719 Duursma, R. A.: YplantQMC: plant architectural analysis with Yplant and
720 QuasiMC, 2014.

721 Duursma, R. A.: Plantecophys - An R Package for Analysing and Modelling Leaf Gas
722 Exchange Data, PLOS ONE, 10, e0143346, 10.1371/journal.pone.0143346, 2015.

723 Farquhar, G. D., Von Caemmerer, S., and Berry, J. A.: A biochemical model of
724 photosynthetic carbon dioxide assimilation in leaves of 3-carbon pathway species, Planta,
725 149, 78-90, 1980.

726 Fatichi, S., Leuzinger, S., and Körner, C.: Moving beyond photosynthesis: from carbon
727 source to sink-driven vegetation modeling, New Phytologist, 201, 1086-1095,
728 10.1111/nph.12614, 2014.

729 Fatichi, S., Pappas, C., and Ivanov, V. Y.: Modeling plant–water interactions: an
730 ecohydrological overview from the cell to the global scale, Wiley Interdisciplinary Reviews:
731 Water, 3, 327-368, doi:10.1002/wat2.1125, 2016.

732 Friend, A. D., Lucht, W., Rademacher, T. T., Keribin, R., Betts, R., Cadule, P., Ciais, P.,
733 Clark, D. B., Dankers, R., Falloon, P. D., Ito, A., Kahana, R., Kleidon, A., Lomas, M. R.,
734 Nishina, K., Ostberg, S., Pavlick, R., Peylin, P., Schaphoff, S., Vuichard, N., Warszawski, L.,
735 Wiltshire, A., and Woodward, F. I.: Carbon residence time dominates uncertainty in
736 terrestrial vegetation responses to future climate and atmospheric CO2, Proceedings of the
737 National Academy of Sciences, 111, 3280-3285, 10.1073/pnas.1222477110, 2014.

738 Gunderson, C. A., and Wullschleger, S. D.: Photosynthetic acclimation in trees to rising
739 atmospheric CO_2: a broader perspective, Photosynthesis Research, 39, 369-388, 1994.

740 Hamilton, E. W., Frank, D. A., Hinchey, P. M., and Murray, T. R.: Defoliation induces root
741 exudation and triggers positive rhizospheric feedbacks in a temperate grassland, Soil Biology
742 and Biochemistry, 40, 2865-2873, https://doi.org/10.1016/j.soilbio.2008.08.007, 2008.

743 Hartmann, H., McDowell, N. G., and Trumbore, S.: Allocation to carbon storage pools in
744 Norway spruce saplings under drought and low CO2, Tree Physiol., 35, 243-252,
745 10.1093/treephys/tpv019, 2015.

746 Hartmann, H., and Trumbore, S.: Understanding the roles of nonstructural carbohydrates in
747 forest trees – from what we can measure to what we want to know, New Phytologist, 211,
748 386-403, doi:10.1111/nph.13955, 2016.

749 Hartmann, H., Adams, H. D., Hammond, W. M., Hoch, G., Landhäusser, S. M., Wiley, E.,
750 and Zaehle, S.: Identifying differences in carbohydrate dynamics of seedlings and mature
751 trees to improve carbon allocation in models for trees and forests, Environ. Exp. Bot.,
752 https://doi.org/10.1016/j.envexpbot.2018.03.011, 2018.

753 Hughes, I. G., and Hase, T. P. A.: Measurements and their Uncertainties A Practical Guide to
754 Modern Error Analysis, Oxford University Press, Oxford, UK, 2010.

755 Jain, A. K., and Yang, X.: Modeling the effects of two different land cover change data sets
756 on the carbon stocks of plants and soils in concert with CO2 and climate change, Global
757 Biogeochemical Cycles, 19, n/a-n/a, 10.1029/2004GB002349, 2005.

758 Karst, J., Gaster, J., Wiley, E., and Landhäusser, S. M.: Stress differentially causes roots of
759 tree seedlings to exude carbon, Tree Physiol., 37, 154-164, 10.1093/treephys/tpw090, 2017.

760 Klein, T., and Hoch, G.: Tree carbon allocation dynamics determined using a carbon mass
761 balance approach, New Phytologist, 205, 147-159, doi:10.1111/nph.12993, 2015.

762 Knorr, W., and Kattge, J.: Inversion of terrestrial ecosystem model parameter values against
763 eddy covariance measurements by Monte Carlo sampling, Glob. Change Biol., 11, 1333-
764 1351, 2005.

765 Körner, M., Waser, B., Rehmann, R., and Reubi, J. C.: Early over-expression of GRP
766 receptors in prostatic carcinogenesis, The Prostate, 74, 217-224, 10.1002/pros.22743, 2014.

767 Law, R. M., Kowalczyk, E. A., and Wang, Y. P.: Using atmospheric CO2 data to assess a
768 simplified carbon-climate simulation for the 20th century, Tellus Ser. B-Chem. Phys.
769 Meteorol., 58, 427-437, 2006.

770 Maina, G. G., Brown, J. S., and Gersani, M.: Intra-plant versus inter-plant root competition in
771 beans: avoidance, resource matching or tragedy of the commons, Plant Ecology, 160, 235-
772 247, 2002.

773 Makela, A., Landsberg, J., Ek, A. R., Burk, T. E., Ter-Mikaelian, M., Agren, G. I., Oliver, C.
774 D., and Puttonen, P.: Process-based models for forest ecosystem management: current state of
775 the art and challenges for practical implementation, Tree Physiol., 20, 289-298, 2000.

776 McConnaughay, K. D. M., and Bazzaz, F. A.: Is Physical Space a Soil Resource?, Ecology,
777 72, 94-103, 10.2307/1938905, 1991.

778 McMurtrie, R., and Wolf, L.: A model of competition between trees and grass for radiation,
779 water and nutrients, Annals of Botany (London), 52, 449-458, 1983.

780 Medlyn, B. E., Duursma, R. A., Eamus, D., Ellsworth, D. S., Prentice, I. C., Barton, C. V. M.,
781 Crous, K. Y., de Angelis, P., Freeman, M., and Wingate, L.: Reconciling the optimal and
782 empirical approaches to modelling stomatal conductance, Glob. Change Biol., 17, 2134-2144,
783 10.1111/j.1365-2486.2010.02375.x, 2011.

784 Metropolis, N., Rosenbluth, A. W., Rosenbluth, M. N., Teller, A. H., and Teller, E.: Equation
785 of State Calculations by Fast Computing Machines, J. Chem. Phys., 21, 10.1063/1.1699114,
786 1953.

787 Mitchell, R. J., Liu, Y., O'Brien, J. J., Elliott, K. J., Starr, G., Miniat, C. F., and Hiers, J. K.:
788 Future climate and fire interactions in the southeastern region of the United States, Forest
789 Ecology and Management, 327, 316-326, https://doi.org/10.1016/j.foreco.2013.12.003, 2014.

790 Müller, C., Cramer, W., Hare, W. L., and Lotze-Campen, H.: Climate change risks for
791 African agriculture, Proceedings of the National Academy of Sciences, 108, 4313-4315,
792 10.1073/pnas.1015078108, 2011.

Nikinmaa, E., Sievänen, R., and Hölttä, T.: Dynamics of leaf gas exchange, xylem and phloem transport, water potential and carbohydrate concentration in a realistic 3-D model tree crown, Annals of Botany, 114, 653-666, 10.1093/aob/mcu068, 2014.

Paul, M. J., and Foyer, C. H.: Sink regulation of photosynthesis, J Exp Bot, 52, 1383-1400, 2001.

Pinnington, E. M., Casella, E., Dance, S. L., Lawless, A. S., Morison, J. I. L., Nichols, N. K., Wilkinson, M., and Quaife, T. L.: Investigating the role of prior and observation error correlations in improving a model forecast of forest carbon balance using Four-dimensional Variational data assimilation, Agricultural and Forest Meteorology, 228-229, 299-314, https://doi.org/10.1016/j.agrformet.2016.07.006, 2016.

Poorter, H., Bühler, J., van Dusschoten, D., Climent, J., and Postma, J. A.: Pot size matters: a meta-analysis of the effects of rooting volume on plant growth, Funct Plant Biol, 39, 839-850, 10.1071/fp12049, 2012a.

Poorter, H., Niklas, K. J., Reich, P. B., Oleksyn, J., Poot, P., and Mommer, L.: Biomass allocation to leaves, stems and roots: meta-analyses of interspecific variation and environmental control, New Phytologist, 193, 30-50, 10.1111/j.1469-8137.2011.03952.x, 2012b.

Pugh, T. A. M., Müller, C., Arneth, A., Haverd, V., and Smith, B.: Key knowledge and data gaps in modelling the influence of CO2 concentration on the terrestrial carbon sink, Journal of Plant Physiology, 203, 3-15, https://doi.org/10.1016/j.jplph.2016.05.001, 2016.

Quaife, T., Lewis, P., De Kauwe, M., Williams, M., Law, B. E., Disney, M., and Bowyer, P.: Assimilating canopy reflectance data into an ecosystem model with an Ensemble Kalman Filter, Remote Sens. Environ., 112, 1347-1364, https://doi.org/10.1016/j.rse.2007.05.020, 2008.

Reich, P. B.: Key canopy traits drive forest productivity, Proceedings of the Royal Society B: Biological Sciences, 10.1098/rspb.2011.2270, 2012.

819 Richardson, A. D., Williams, M., Hollinger, D. Y., Moore, D. J. P., Dail, D. B., Davidson, E.
820 A., Scott, N. A., Evans, R. S., Hughes, H., Lee, J. T., Rodrigues, C., and Savage, K.:
821 Estimating parameters of a forest ecosystem C model with measurements of stocks and fluxes
822 as joint constraints, Oecol., 164, 25-40, 10.1007/s00442-010-1628-y, 2010.

823 Richardson, A. D., Carbone, M. S., Keenan, T. F., Czimczik, C. I., Hollinger, D. Y.,
824 Murakami, P., Schaberg, P. G., and Xu, X. M.: Seasonal dynamics and age of stemwood
825 nonstructural carbohydrates in temperate forest trees, New Phytologist, 197, 850-861,
826 10.1111/nph.12042, 2013.

827 Robbins, N. S., and Pharr, D. M.: Effect of Restricted Root Growth on Carbohydrate
828 Metabolism and Whole Plant Growth of Cucumis sativus L, Plant Physiol., 87,
829 409-413, 10.1104/pp.87.2.409, 1988.

830 Rowland, L., Hill, T. C., Stahl, C., Siebicke, L., Burban, B., Zaragoza-Castells, J., Ponton, S.,
831 Bonal, D., Meir, P., and Williams, M.: Evidence for strong seasonality in the carbon storage
832 and carbon use efficiency of an Amazonian forest, Glob. Change Biol., 20, 979-991,
833 10.1111/gcb.12375, 2014.

834 Running, S. W., and Gower, S. T.: FOREST-BGC, A general model of forest ecosystem
835 processes for regional applications. II. Dynamic carbon allocation and nitrogen budgets1,
836 Tree Physiol., 9, 147-160, 10.1093/treephys/9.1-2.147, 1991.

837 Sage, R. F.: Acclimation of photosynthesis to increasing atmospheric CO_2: the gas-exchange
838 perspective, Photosynthesis Research, 39, 351-368, 1994.

839 Sala, A., Woodruff, D. R., and Meinzer, F. C.: Carbon dynamics in trees: feast or famine?,
840 Tree Physiol., 32, 764-775, 10.1093/treephys/tpr143, 2012.

841 Schiestl-Aalto, P., Kulmala, L., Mäkinen, H., Nikinmaa, E., and Mäkelä, A.: CASSIA – a
842 dynamic model for predicting intra-annual sink demand and interannual growth variation in
843 Scots pine, New Phytologist, 206, 647-659, 10.1111/nph.13275, 2015.

844 Schwarz, G.: Estimating the Dimension of a Model, Ann. Statist., 6, 461-464,
845 10.1214/aos/1176344136, 1978.

846 Thornley, J. H. M., and Cannell, M. G. R.: Modelling the Components of Plant Respiration:
847 Representation and Realism, Annals of Botany, 85, 55-67, 10.1006/anbo.1999.0997, 2000.

848 Thornton, P. E., Lamarque, J.-F., Rosenbloom, N. A., and Mahowald, N. M.: Influence of
849 carbon-nitrogen cycle coupling on land model response to CO2 fertilization and climate
850 variability, Global Biogeochemical Cycles, 21, n/a-n/a, 10.1029/2006GB002868, 2007.

851 Van Oijen, M.: Bayesian Calibration (BC) and Bayesian Model Comparison (BMC) of
852 Process-Based Models: Theory, Implementation and Guidelines, 2008.

853 Villar, R., and Merino, J.: Comparison of leaf construction costs in woody species with
854 differing leaf life-spans in contrasting ecosystems, New Phytologist, 151, 213-226,
855 10.1046/j.1469-8137.2001.00147.x, 2001.

856 Wiley, E., and Helliker, B.: A re-evaluation of carbon storage in trees lends greater support
857 for carbon limitation to growth, New Phytologist, 195, 285-289, 10.1111/j.1469-
858 8137.2012.04180.x, 2012.

859 Williams, M., Schwarz, P. A., Law, B. E., Irvine, J., and Kurpius, M. R.: An improved
860 analysis of forest carbon dynamics using data assimilation, Glob. Change Biol., 11, 89-105,
861 2005.

862 Zaehle, S., and Friend, A. D.: Carbon and nitrogen cycle dynamics in the O-CN land surface
863 model: 1. Model description, site-scale evaluation, and sensitivity to parameter estimates,
864 Global Biogeochemical Cycles, 24, n/a-n/a, 10.1029/2009GB003521, 2010.

865 Zobitz, J. M., Desai, A. R., Moore, D. J. P., and Chadwick, M. A.: A primer for data
866 assimilation with ecological models using Markov Chain Monte Carlo (MCMC), Oecol., 167,
867 599, 10.1007/s00442-011-2107-9, 2011.
868